UltraRapid Communication

Calcium Dynamics in Cortical Astrocytes and Arterioles During Neurovascular Coupling

Jessica A. Filosa, Adrian D. Bonev, Mark T. Nelson

Abstract—Neuronal activity in the brain is thought to be coupled to cerebral arterioles (functional hyperemia) through Ca^{2+} signals in astrocytes. Although functional hyperemia occurs rapidly, within seconds, such rapid signaling has not been demonstrated in situ, and Ca^{2+} measurements in parenchymal arterioles are still lacking. Using a laser scanning confocal microscope and fluorescence Ca^{2+} indicators, we provide the first evidence that in a brain slice preparation, increased neuronal activity by electrical stimulation (ES) is rapidly signaled, within seconds, to cerebral arterioles and is associated with astrocytic Ca^{2+} waves. Smooth muscle cells in parenchymal arterioles exhibited Ca^{2+} and diameter oscillations ("vasomotion") that were rapidly suppressed by ES. The neuronal-mediated Ca^{2+} rise in cortical astrocytes was dependent on intracellular (inositol trisphosphate [IP_3]) and extracellular voltage-dependent Ca^{2+} channel sources. The Na^+ channel blocker tetrodotoxin prevented the rise in astrocytic $[Ca^{2+}]_i$ and the suppression of Ca^{2+} oscillations in parenchymal arterioles to ES, indicating that neuronal activity was necessary for both events. Activation of metabotropic glutamate receptors in astrocytes significantly decreased the frequency of Ca^{2+} oscillations in parenchymal arterioles. This study supports the concept that astrocytic Ca^{2+} changes signal the cerebral microvasculature and indicate the novel concept that this communication occurs through the suppression of arteriolar $[Ca^{2+}]_i$ oscillations and corresponding vasomotion. The full text of this article is available online at http://circres.ahajournals.org. **(*Circ Res*. 2004;95:e73-e81.)**

Key Words: astrocytes ■ calcium ■ functional hyperemia ■ neurovascular ■ myocytes

Normal brain function requires an exquisite and finely tuned interaction of numerous cell types. Working neurons must receive a proper supply of oxygen and glucose in a timely and locally restricted manner. In the brain, this is accomplished by a rapid increase in local cerebral blood flow termed functional hyperemia. Blood flow to the brain is provided by extracerebral and intracerebral arteries/arterioles. In general, extracerebral vessels are innervated by peripheral nerves (extrinsic innervation).[21] On the other hand, parenchymal microvessels are primarily regulated by local interneurons and neuronal terminals from a central origin (intrinsic innervation).[11,26] These arterioles are also regulated by the action of astrocytes and, to some extent, by peripheral nerves that penetrate the brain parenchyma.[19]

Astrocytes have been proposed to signal arterioles to dilate in response to increased neuronal activity.[57,58] This attractive hypothesis has intensified the search for the mechanisms that underlie neurovascular coupling. Astrocytes respond to an increase in synaptic activity with a rise in $[Ca^{2+}]_i$,[1,12] which, in turn, travels to nearby vessels.[17,57] This astrocytic Ca^{2+} wave appears to be an element that contributes to the vasodilatory response of cerebral arterioles to increased neuronal activity.[57] However, in a recent study, an opposite response to astrocytic Ca^{2+} activation was observed in the cerebral microvessels. In response to the release of caged Ca^{2+} in astrocytes, microvessels without tone constricted.[36] The vasoconstriction was attributed to the inhibition of Ca^{2+}-activated potassium channels by 20-hydroxyeicosatetraenoic acid (20-HETE).[36] Furthermore, astrocytes have also been shown to synthesize and release a number of vasoactive substances such as NO,[31,54] prostacyclins, epoxyeicosatrienoic acids (EETs), glutamate, adenosine, and ATP,[3,23,31,51,56–58] making them potential candidates mediating neurovascular coupling. In addition to these potential signals, astrocytes have also been implicated in shunting K^+ ions from areas of high concentration around the active synapse to areas of lower concentration around the astrocytic endfoot,[41] to participate in functional hyperemia.[4,42] Nonetheless, despite the growing cellular evidence for neurovascular coupling, a number of significant gaps in our understanding remain. First, rapid vasodilatory communication (≈1 to 2 seconds) from neurons to arterioles, which is expected and required during functional hyperemia,[9] has not been demonstrated. Second, intracellular Ca^{2+} measurements in vascular smooth muscle cells (VSMCs) in the arterioles in response to increased neuronal activity are completely lacking.[40]

To examine neurovascular coupling in the brain, we developed an approach to simultaneously measure intracellular Ca^{2+} changes in astrocytes and parenchymal arterioles in brain slices with relative high temporal and spatial resolution. Using this approach, we detected Ca^{2+} oscillations in indi-

Original received August 17, 2004; resubmission received October 6, 2004; accepted October 7, 2004.

From the Department of Pharmacology, College of Medicine, University of Vermont, Burlington.

Correspondence to Mark T. Nelson, PhD, Professor and Chair, Department of Pharmacology, University of Vermont, Given Building, Room B-333, 89 Beaumont Ave, Burlington VT 05405-0068. E-mail Mark.Nelson@uvm.edu

Circulation Research **is available at http://www.circresaha.org** **DOI: 10.1161/01.RES.0000148636.60732.2e**

vidual myocytes in these arterioles. On neuronal stimulation, Ca^{2+} oscillations in the arterioles were suppressed within the period of one Ca^{2+} oscillation (<2 seconds) in the arteriole and coincided with a Ca^{2+} wave through the adjacent astrocyte. Metabotropic glutamate agonists mimicked the effects of neuronal stimulation. These results support the concept that neurovascular coupling occurs rapidly, with the participation of Ca^{2+} signaling through astrocytes, to suppress Ca^{2+} oscillations and vasomotion in parenchymal arterioles.

Materials and Methods

Slice Preparation

Cortical slices were prepared from neonatal (P7–P10) and juvenile (>20 days old) Sprague-Dawley rats following reviewed and approved protocols by the Office of Animal Care Management at the University of Vermont. Whereas experiments conducted for Figures 1, 2, and 3 were performed from neonatal rat brain slices, the rest of the experiments were done in juvenile rats. The image resolution of astrocytic Ca^{2+} waves was superior in neonatal rats compared with older animals. The cortex was rapidly removed and placed onto a vibratome (Leica VT 1000S) used to cut ≈200-μm-thick coronal slices into artificial cerebrospinal fluid (aCSF; for composition, see below) at 4°C to 6°C. Slices were immediately incubated at room temperature in aCSF equilibrated with 95%O_2/5%CO_2, pH≈7.45, until needed.

Ca^{2+} Imaging

Ca^{2+} imaging was performed using the Solamere confocal scanning unit (QLC 100) in combination with a high-sensitivity, high-resolution camera (GEN IV ICCD). The confocal unit was attached to a Nikon microscope (Eclipse 600). Briefly, cortical slices were incubated at room temperature in aCSF containing 10 μmol/L Fluo-4 AM and pluronic acid (2.5 μg/mL). After a two- to three-hour incubation period, slices were washed and placed in aCSF (at room temperature) until needed. Using this loading protocol, we were able to visualize Ca^{2+} transients in astrocytes and VSMCs. In accordance with previous reports, under these conditions, neurons did not load sufficiently for Ca^{2+} detection.[46,55] At the time of the experiment, a slice was transferred to a perfusion chamber on the microscope and held with a nylon grid and continuously superfused with aCSF maintained at 35°C to 37°C. Parenchymal microvessels were visualized with a ×60 water-dipping objective (NA 1.0). Fluorescence images were obtained using a krypton/argon laser at 488 nm and emitted light at >495 nm. Images were acquired at 60 or 30 frames per second for 40 to 60 seconds, depending on the experimental protocol.

Video Imaging

Video microscopy was used to determine the rate of vasomotion and that of diameter changes using infrared differential interference contrast (DIC) with a charge-coupled device Hamamatsu camera. Images were acquired at 12 images per second and stored on a computer hard drive for later analysis. Changes in internal diameter throughout the experiment were determined from the distance between two set point values across the arteriole.

Electrical Stimulation

Neuronal electrical stimulation (ES) was performed using either electrical field stimulation (EFS) or focal stimulation (FS). EFS was induced with a pair of platinum wires placed parallel to the brain slice (10 to 50 Hz; 0.3-millisecond pulses for 5 to 8 seconds). To verify that the responses observed in the slice preparation during EFS were also possible in response to a local stimulus, experiments were also performed using FS using a lower-voltage protocol. FS was conducted with a pair of concentric bipolar electrodes placed a few micrometers away from the vessel wall, and if possible, in the vicinity of a nearby astrocyte. The stimulation protocol (amount of voltage needed) varied depending on the distance between the electrodes and the cellular targets.

Solutions

The composition of the aCSF (in mmol/L): 5 KCl, 124 NaCl, 1.3 $MgSO_4$, 26 $NaHCO_3$, 1.24 KH_2PO_4, 10 glucose, 2.4 $CaCl_2$, and 400 μmol/L L-ascorbic acid, equilibrated with 95% O_2/5% CO_2. Ascorbic acid was added to the solution to reduce cell swelling associated with oxidative stress.[6]

Drugs

The metabotropic glutamate receptor (mGluR) antagonists (*RS*)-1-aminoindan-1,5-dicarboxylic acid (AIDA) and 2-methyl-6-(phenylethynyl)pyridine hydrochloride (MPEP) and the inositol trisphosphate (IP_3) receptor blocker 2-aminoethoxydiphenylborate (2-APB) were obtained from Tocris Cookson, and the mGluR agonist (±)-1-aminocyclopentane-*trans*-1,3-dicarboxylic acid (*t*-ACPD) was obtained from Sigma. All other drugs used were obtained from Sigma: thromboxane A_2 receptor agonist 9, 11-dideoxy-11α, 9α-epoxymethanoprostaglandin $F_{2\alpha}$ (U46619), tetrodotoxin (TTX), and nifedipine.

Data Analysis

Ca^{2+} image experiments were analyzed with custom software created by Dr Adrian D. Bonev in our laboratory. Fractional fluorescence (F/F_0) was determined by dividing the fluorescence intensity (F) within a region of interest (ROI) by a baseline fluorescence value (F_0) determined from 50 images showing no activity. The frequency of Ca^{2+} oscillations was determined by placing an ROI (10×10 pixels or 2.5×2.5 μm) on a cell showing Ca^{2+} oscillations. The number of peaks over a given time was automatically detected from oscillations crossing a set threshold value (>1.15 F/F_0).

Statistics

Data are expressed as mean±SEM. Differences between two means were determined using Student *t* test. Statistical significance was tested at 95% ($P<0.05$) confidence level.

Results

Calcium Signaling in Astrocytes in Close Apposition to Parenchymal Arterioles

Unlike extracerebral/pial and systemic arteries, parenchymal arterioles are surrounded by astrocytic processes ("endfeet").[14] Activated neurons release glutamate, which acts through mGluRs to stimulate phospholipase C activity and increase IP_3 levels in nearby astrocytes.[8] The resulting IP_3 receptor (IP_3R)–mediated Ca^{2+} wave travels through the astrocyte to the endfoot, presumably signaling the parenchymal arterioles to dilate.[57] We found that EFS leads to a rise in $[Ca^{2+}]_i$ in several (≈3 to 5) astrocytes, imaged within the same optical field, that reached a peak in each case within a few seconds from each other (n=5; Figure 1A and 1B). On several occasions, we were able to detect the Ca^{2+} wave spread from the astrocytic soma to the endfeet along the vessel wall (supplemental Movies I and II, available in the online data supplement at http://circres.ahajournals.org). Figure 1 illustrates the short delay (<3 seconds) between $[Ca^{2+}]_i$ peaking in the soma and the endfoot. It was not possible to determine whether the endfoot and soma correspond to the same astrocyte because they were often in different optical planes. Nevertheless, there was a clear delay between the rise in Ca^{2+} at the soma of astrocytes and along the vessel wall or endfeet (Figure 1; also see Figure 6). Repetitive EFS did not

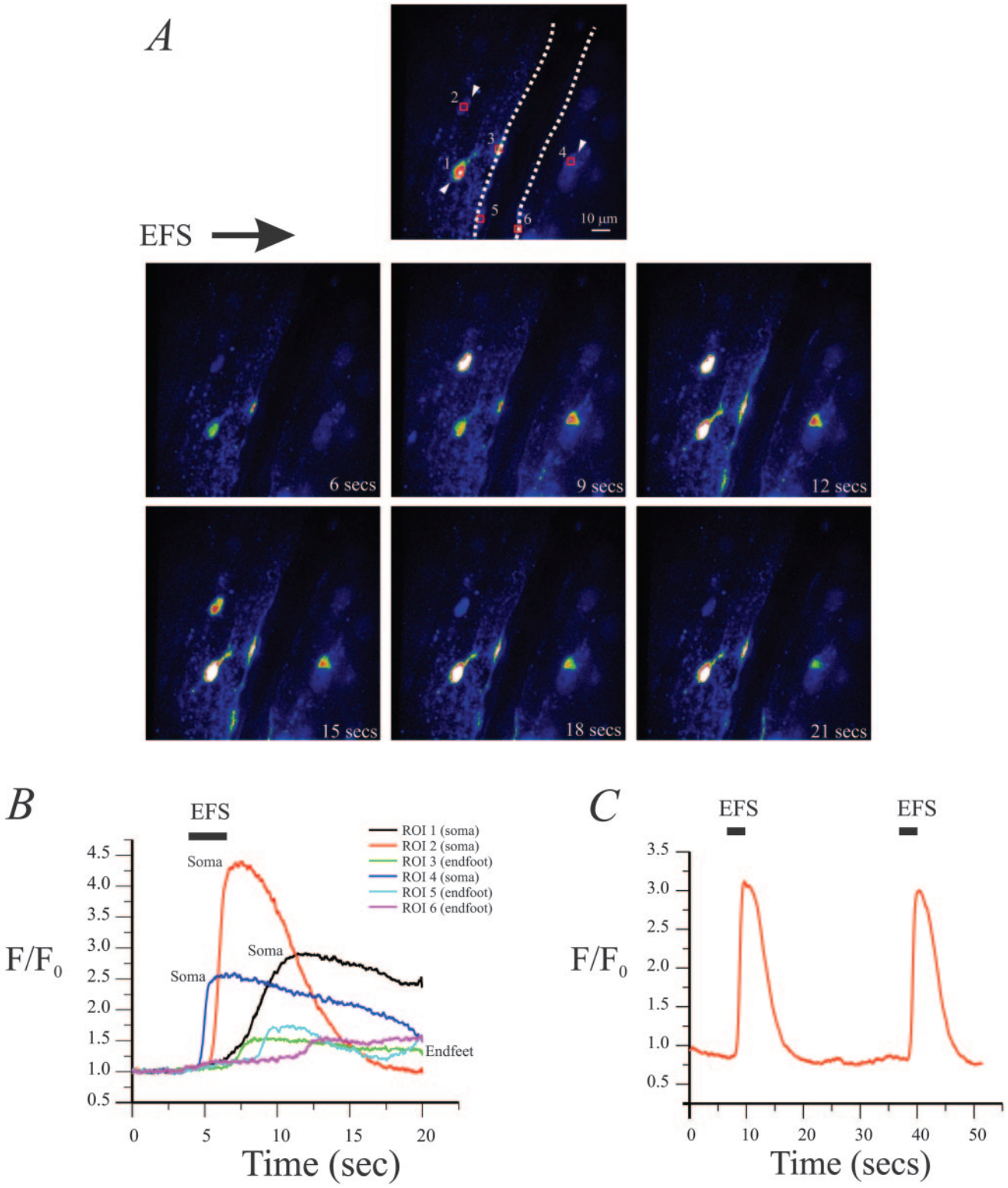

Figure 1. Ca^{2+} transient in cortical astrocytes in response to EFS. A, Representative images from a cortical brain slice in response to EFS. The dashed line in the first image outlines a cerebral arteriole, whereas the arrowhead shows the position of nearby cortical astrocytes. EFS had already started in image 2 (6 seconds). B, Transient Ca^{2+} changes induced by EFS from the soma of three astrocytes (ROIs 1, 2, and 4) and from the endfeet along the vessel wall (ROIs 3, 5, and 6), the top right panel indicates the corresponding ROI. C, Representative Ca^{2+} changes from a cortical astrocyte in response to two EFSs.

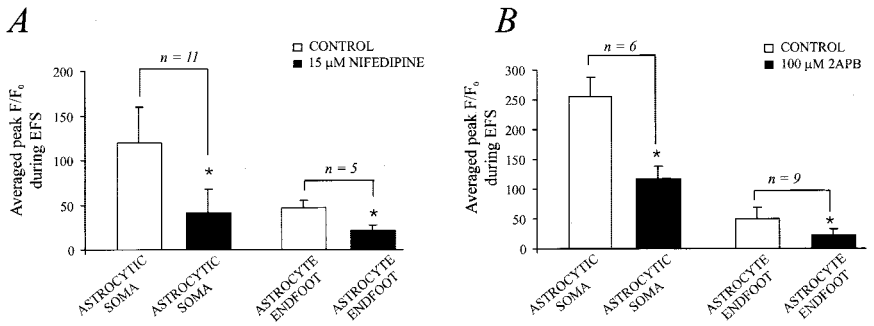

Figure 2. L-type calcium channel and IP_3R inhibition reduces the rise in cortical astrocyte $[Ca^{2+}]_i$ to EFS. A, Inhibition of the transient rise in Ca^{2+} in cortical astrocytes by the L-type channel blocker nifedipine (15 μmol/L for 15 minutes). B, Inhibition of the transient rise in Ca^{2+} in cortical astrocytes in the presence of the IP_3 channel blocker 2-APB (100 μmol/L for 15 minutes). Ca^{2+} transients were recorded from the cell soma and from the endfeet along the vessel wall.

change the profile of the rise in Ca^{2+} in cortical astrocytes (Figure 1C).

The EFS-induced rise in astrocytic $[Ca^{2+}]_i$ involved L-type voltage-dependent Ca^{2+} channels and IP_3Rs (Figure 2). The L-type Ca^{2+} channel blocker nifedipine (15 μmol/L) reduced the EFS-induced rise in $[Ca^{2+}]_i$ in the astrocytic soma and the endfoot by 51±10% (n=11; three experiments) and 49±16% (n=5; three animals), respectively (Figure 2A). These effects could reflect inhibition of L-type Ca^{2+} channels in the neurons and astrocytes.[13,5,33]

The rise in astrocytic $[Ca^{2+}]_i$ likely also involves activation of IP_3Rs.[35,43] Therefore, the effects of the IP_3R blocker 2-APB (100 μmol/L) were tested. This blocker caused a reduction in the EFS-induced rise in $[Ca^{2+}]_i$ in the astrocytic soma and endfoot by 55±13% (n=6; three experiments) and 44±10% (n=9; three animals), respectively (Figure 2B).

To verify that EFS-induced rise in Ca^{2+} indeed reflected a synaptically mediated event, we recorded Ca^{2+} changes in the presence of the Na^+ channel blocker TTX or synaptic blockade media (low extracellular Ca^{2+} [0.24 mmol/L] and EGTA [1 mmol/L]). The EFS-induced rise in $[Ca^{2+}]_i$ was significantly inhibited in the astrocyte soma 92±9% (n=9; three animals) and along the vessel wall 63±16% (n=9; three animals) in the presence of 1 μmol/L TTX. Similar results were obtained in the presence of synaptic blockade media (0.24 mmol/L Ca^{2+}, 1 mmol/L EGTA), which inhibited the EFS-induced increase in $[Ca^{2+}]_i$ at the soma and along the vessel wall by 99±0.3% (n=8; three animals) and 94±2% (n=7; three animals), respectively (Figure 3A and 3B).

Calcium Dynamics in Parenchymal Arterioles

Intracellular Ca^{2+} signaling in parenchymal arterioles has a central role in functional hyperemia. We found that parenchymal arterioles in brain slices exhibit oscillations in intracellular Ca^{2+} (Figure 4; supplemental Movie III) and diameter (vasomotion) in the absence of exogenous agents (n=3), a feature common to many types of vascular beds including the cerebral vasculature.[18,38] To maintain stable vasomotion and Ca^{2+} oscillations in parenchymal arterioles during the course of the experiments, a thromboxane A_2 agonist (U46619; 100 nmol/L) was included in the superfusate.[7] Synchronized Ca^{2+} oscillations in individual myocytes from a single arteriole were also reflected in diameter oscillations (supplemental Movie III). Ca^{2+} oscillations were characterized by having a mean frequency of 0.18±0.02 Hz with a corresponding mean amplitude of F/F_0 1.35±0.03, a duration of 1.09±0.08 seconds, and a half time of decay of 0.64±0.05 seconds (n=19 myocytes from 6 arterioles).

Neuronal Activity Inhibits Ca^{2+} Oscillations in Parenchymal Microvessels

To examine the relationship between astrocytic and parenchymal arteriolar Ca^{2+}, simultaneous measurements of $[Ca^{2+}]_i$ in both cell types were performed. FS or EFS significantly reduced the frequency of Ca^{2+} oscillations in myocytes by 92±5% (n=25; 5 animals; Figure 5). In a different arteriole, where the same protocol was used as during Ca^{2+} imaging, FS resulted in the cessation of vasomotion viewed with DIC (n=3; three animals; Figure 5C; supplemental Movie IV).

Our results suggest the novel concept that neuronal-to-microvessel communication involves an elevation of astrocytic $[Ca^{2+}]_i$ that leads to a suppression of arteriolar Ca^{2+} oscillations and vasomotion, and hence vasodilation. To explore this issue further, intracellular Ca^{2+} was measured simultaneously in adjacent astrocytes and arterioles (n=4) as depicted in Figure 6. The EFS or FS-induced rise in astrocytic

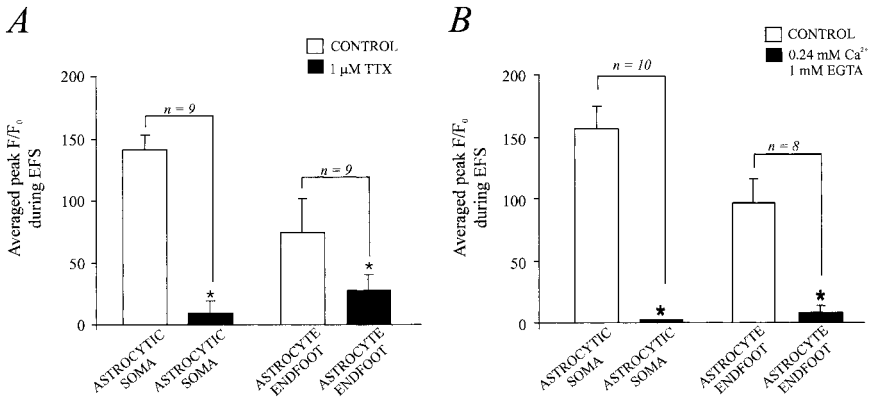

Figure 3. Synaptic blockade abrogates the EFS-induced Ca^{2+} changes in cortical astrocytes. A, Inhibition of Ca^{2+} changes in cortical astrocytes induced by EFS in the presence of 1 μmol/L TTX (5 to 10 minutes). B, Inhibition of Ca^{2+} changes in cortical astrocytes induced by EFS in the presence of synaptic blockade media (10 minutes). Ca^{2+} transients were recorded from the cell soma and from the endfeet along the vessel wall.

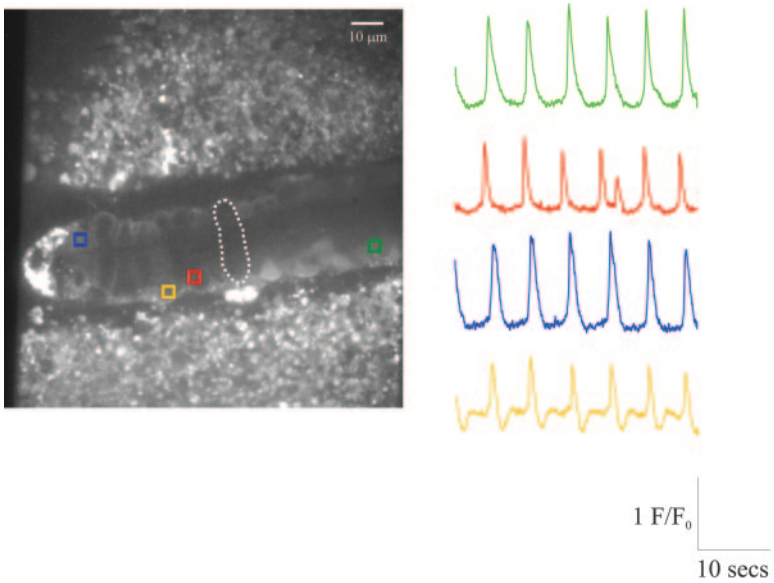

Figure 4. Spontaneous Ca^{2+}oscillations in parenchymal arterioles. Synchronized Ca^{2+}oscillations in myocytes from a parenchymal arteriole in the absence of the thromboxane A_2 receptor agonist U46619. Ca^{2+} was measured in the colored boxes, and F/F_0 is displayed on the right panel. The dotted line outlines an individual myocyte in the parenchymal arteriole.

$[Ca^{2+}]_i$ coincided with a suppression of arteriolar $[Ca^{2+}]_i$ oscillations, which returned during the decay of $[Ca^{2+}]_i$ in the astrocytes. (Supplemental Movie V illustrates a rise in Ca^{2+} in the astrocyte immediately preceding the suppression of Ca^{2+} oscillations in the arteriole.)

To verify that the suppression of parenchymal arteriolar $[Ca^{2+}]_i$ oscillation was indeed associated with increased neuronal activity, the effects of the Na^+ channel blocker TTX (1 μmol/L) were examined. In the presence of TTX, the EFS-induced elevation of astrocytic $[Ca^{2+}]_i$ and the suppression of arteriolar $[Ca^{2+}]_i$ oscillations were abrogated (n=6; six animals; Figure 7). Furthermore, TTX blocked the transient rise in $[Ca^{2+}]_i$ in astrocytes (Figure 7A, first trace), supporting the role of astrocytes in the communication of synaptic activity and suppression of arteriolar $[Ca^{2+}]_i$ (Figure 7, second and third trace).

Effect of mGluR Activation on Myocyte Ca^{2+} Oscillations

It has been proposed that neurovascular coupling may be mediated by the activation of group I mGluRs (mGluR I) after neuronal glutamate release.[57] mGluR I include the mGluR1 and mGluR5 subtypes.[47] Activation of mGluRs results in the rise of $[Ca^{2+}]_i$ and the subsequent release of vasoactive substances from these cells.[57] We therefore tested whether activation of mGluR altered Ca^{2+} dynamics in parenchymal arterioles. The nonspecific mGluR agonist (*t*-ACPD; 50 μmol/L), which is known to increase Ca^{2+} in cortical astrocytes,[47] suppressed Ca^{2+} oscillations in parenchymal arterioles by 96%±3% (n=14; three animals; Figure 8A). In contrast, the EFS-induced suppression of arteriolar Ca^{2+} oscillations persisted (91%±6% inhibition) in the presence of the mGluR I antagonists (50 μmol/L MPEP and 300 μmol/L AIDA; n=9; two animals; Figure 8B and 8C). However, mGluR I antagonists did not abolish the rise in astrocytic $[Ca^{2+}]$ (Figure 8B and 8C).

Discussion

More than 100 years ago, Roy and Sherrington suggested that the brain possesses mechanisms by which blood supply matches the degree of neuronal activity and proposed the release of vasoactive agents into the extracellular space.[49] Along these lines, the role of astrocytes in neurovascular coupling has been revisited recently. Astrocytes send projections to the synapse and blood vessels.[20,29,50] In fact, the anatomical structure of astrocytes allows them to bridge synaptic activity with local metabolic demand and thus modulate regional blood flow accordingly.[37,51,57] Here, we provide the first measurements of $[Ca^{2+}]_i$ in parenchymal arterioles and the first simultaneous measurements of $[Ca^{2+}]_i$ in astrocytes and parenchymal arterioles in brain slices. In arterioles, smooth muscle cells exhibited Ca^{2+} oscillations, which appear to underlie rhythmic fluctuations in vessel diameter. Furthermore, we provide first demonstration of rapid signaling from neurons to arterioles in situ, consistent with functional hyperemia in vivo. Our results indicate that $[Ca^{2+}]_i$ in astrocytes and arterioles respond in opposite fashion because EFS elevates astrocytic $[Ca^{2+}]_i$ and suppresses arteriolar Ca^{2+} oscillations. These results support the idea of an important role for astrocytes[57] and indicate a novel concept in which functional hyperemia involves the suppression of arteriolar Ca^{2+} oscillations and vasomotion.

In our study, the rise in astrocytic Ca^{2+} was reduced by inhibition of L-type Ca^{2+} channels and IP_3Rs. The Ca^{2+} rise in astrocytes is thought to be attributable to IP_3-mediated Ca^{2+} release from intracellular stores.[8] Our results are in agreement with the view that in cortical brain slices, an increase in synaptic activity results in the release of glutamate, activation of metabotropic glutamate receptors, production of IP_3, and transient rise in intracellular Ca^{2+} through an IP_3-mediated Ca^{2+} process (Figures 2 and 8).[8] This idea is supported by the ability of a mGluR agonist to simulate the effects of EFS and the ability of the IP_3R antagonist to reduce astrocytic $[Ca^{2+}]_i$ transients (Figures 2 and 8).

To date, the role of L-type voltage-dependent Ca^{2+} channels in synaptically mediated astrocytic Ca^{2+} waves has been somewhat controversial. Whereas some studies have shown that inhibition of L-type Ca^{2+} channels suppress the rise in $[Ca^{2+}]_i$ in astrocytes,[28,32] others have suggested the main Ca^{2+}

source during glutamate release (neuronal stimulation) arises from the activation of IP_3Rs.[30,35,43,48] Astrocytes express L-type voltage-dependent Ca^{2+} channels,[5,13,33] suggesting that these channels may play a role under physiological or pathological conditions. In our study, the effect of L-type Ca^{2+} channel inhibition on the EFS-induced rise in astrocytic $[Ca^{2+}]_i$ could be attributed to either a direct effect on astrocytic L-type Ca^{2+} channels or to indirect effect, for example, modulation of neuronal activity[13] or Ca^{2+} filling of the astrocytic Ca^{2+} stores.[24] Nonetheless, our results suggest that modulation of L-type voltage-dependent Ca^{2+} channels can significantly alter neuronal-to-arteriole communication.

Rhythmic contractions (vasomotion) have been observed in a number of vascular beds, including the cerebrovasculature.[18,38] Vasomotion has been associated with a number of physiological functions including blood flow changes in response to metabolic demand.[52] In vivo studies on reflectance imaging have shown the presence of vasomotion in the brain as well as its interruption by increased neuronal activity.[34] In extracerebral arterioles, vasomotion has been attributed to oscillations in membrane potential, which cause

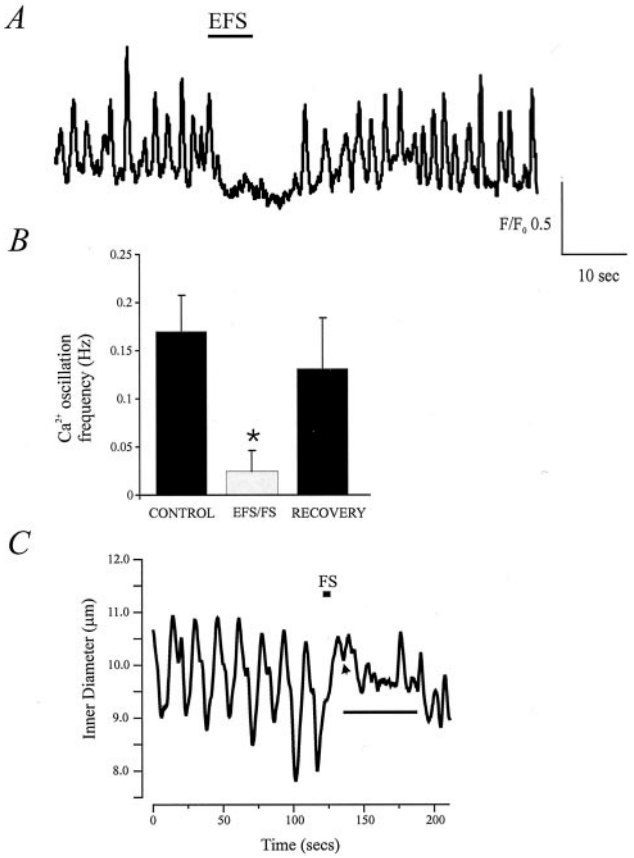

Figure 5. ES-induced inhibition of Ca^{2+} oscillations and diameter in parenchymal arterioles. A, A representative trace showing inhibition of Ca^{2+} oscillations in response to FS. B, Summary data (n=5) showing a significant decrease in the frequency of Ca^{2+} oscillations in myocytes during EFS or FS. C, A representative trace illustrating suppression of vasomotion (diameter oscillations) in different parenchymal arteriole to that shown in A during FS. The bar depicts the duration of the response, starting from the inhibition of the first expected oscillations (arrowhead) after the stimulus (FS).

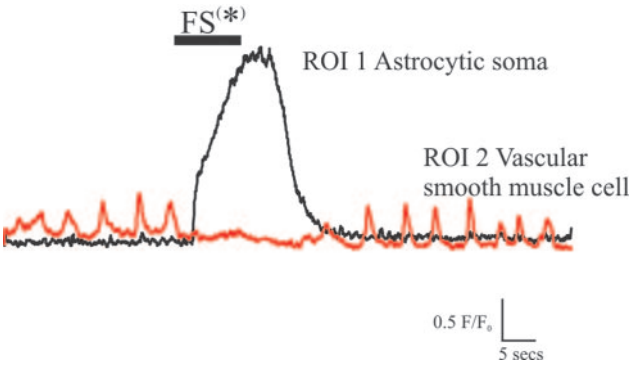

Figure 6. Simultaneous measurements of Ca^{2+} changes in an astrocyte and a myocyte from a parenchymal arteriole in response to FS. Example of Ca^{2+} oscillations from a parenchymal arteriole. ROI 1 (back) corresponds to a distant astrocyte, and ROI 2 (gray) corresponds to vascular cell. The asterisk represents the onset of the FS.

the activation and deactivation of voltage-dependent Ca^{2+} channels, and in turn, leads to oscillations in intracellular Ca^{2+} concentration $[Ca^{2+}]_i$.[22] Consequently, these rhythmic oscillations in $[Ca^{2+}]_i$ and diameter are abolished by inhibition of voltage-dependent Ca^{2+} channels.[22] We found that Ca^{2+} oscillations occurred spontaneously and were maintained by the thromboxane agonist U46619. Because the arterioles in the brain slice are not pressurized, it is likely that

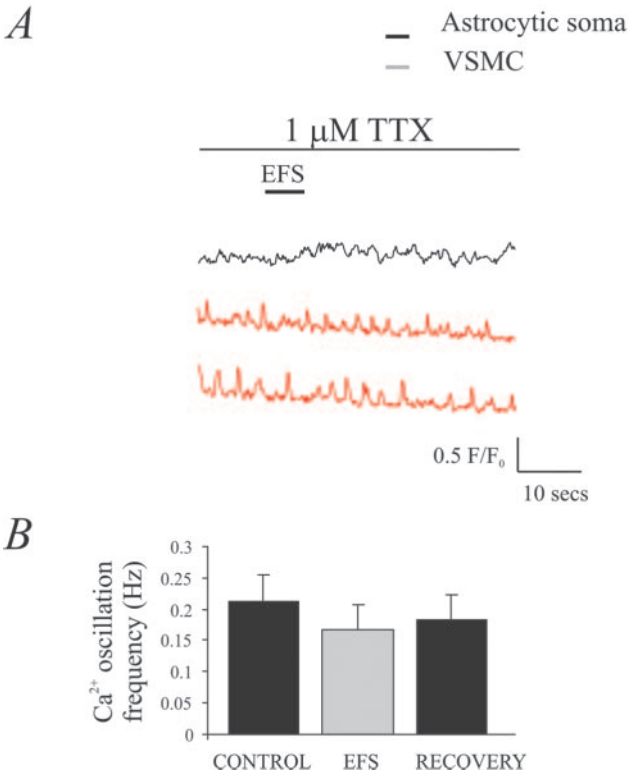

Figure 7. EFS fails to inhibit Ca^{2+} oscillations in myocytes in the presence of TTX. A, Representateve traces showing Ca^{2+} changes in response to EFS in the presence of 1 μmol/L TTX (5 to 10 minutes). EFS failed to induce a significant change in astrocytic $[Ca^{2+}]$ and in the frequency of Ca^{2+} oscillations in the VSMCs (gray; n=6). B, Summary data showing mean values for Ca^{2+} oscillations in myocytes before and during EFS in the presence of 1 μmol/L TTX.

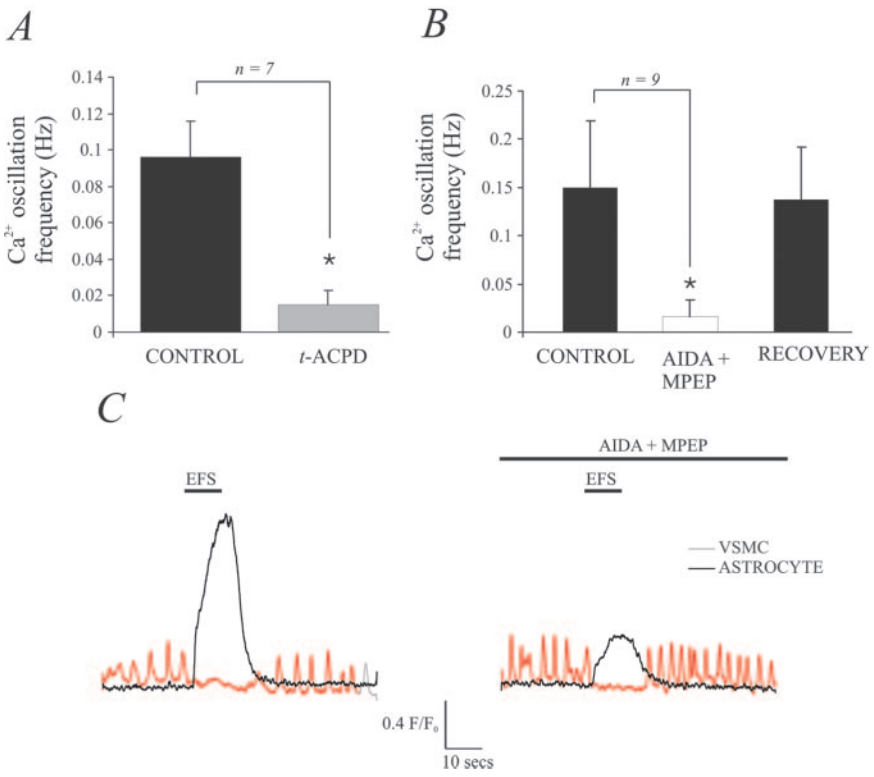

Figure 8. mGluR activation significantly suppresses Ca^{2+} oscillations in parenchymal arterioles. A, Summary data showing a significant decrease in the frequency of Ca^{2+} oscillations in parenchymal arterioles exposed to the mGluR agonist *t*-ACPD (50 μmol/L) for ≈10 minutes. B, Summary data illustrating no changes in the EFS-induced suppression of arteriolar Ca^{2+} oscillations in the presence of the mGluR I antagonists AIDA (300 μmol/L) and MPEP (50 μmol/L) for ≈10 minutes. C, Representative traces showing the EFS-induced suppression of Ca^{2+} oscillations in a parenchymal arteriole (in gray) and the simultaneous rise in astrocytic $[Ca^{2+}]_i$ (in black) in response to EFS (left panel). In the presence of the mGluR antagonists MPEP and AIDA, the EFS-induced suppression of Ca^{2+} oscillations persist, whereas the elevation of astrocytic Ca^{2+} is significantly reduced (right panel).

Ca^{2+} oscillations and vasomotion would be more prominent in pressurized arterioles.[38] A recent report indicated that vasomotion (diameter oscillations) of hippocampal cerebral arterioles is inhibited by stimulation of the Schaeffer collaterals.[7] We provide the first measurement of intracellular $[Ca^{2+}]_i$ in parenchymal arterioles, and that $[Ca^{2+}]$ oscillations are suppressed by neuronal activity.

A number of mechanisms involved in the vasodilation response of cerebral arterioles have been suggested. These include vasodilation as a result of arachadonic acid metabolism and the subsequent release of prostanoids and EETs.[23] In addition, glutamate release from the presynaptic terminal through actions on postsynaptic *N*-methyl-D-aspartate receptors has been shown to induce release of NO.[16] Studies on the potential role of NO and prostanoids in neurovascular coupling are supported by in vitro and in vivo studies, which show attenuation of the functional hyperemic response to neuronal stimulation by inhibitors of neuronal NO (7-nitroindazole) and cyclooxygenase.[2,10,15,25,39,44,53] The lack of full blockade of this response by glutamate receptor antagonists (Figure 8) suggest that multiple mechanisms lead to functional hyperemia in the brain. However, one of the major gaps in the above studies is the lack of direct Ca^{2+} measurements in parenchymal arterioles in association with neuronal activity as well as the time resolution by which neuron-to-vessel communication takes place. Zonta et al reported a significant delay (≈30 to 120 seconds) between neuronal stimulation and vasodilation.[57] Furthermore, their intercellular communication studies[57] suggesting a role for astrocytes in neurovascular coupling were performed in neonatal rats (P9–P15) that contain a large number of immature vessels, which could contribute to the slow response of these vessels.

A recent study by Mulligan and MacVicar raised the interesting possibility that a rise in astrocytic Ca^{2+} is associated with microvascular vasoconstriction and not vasodilation.[36] In their study, the authors point out that the possible mechanism leading to microvascular vasoconstriction is the inhibition of calcium-activated K^+ channels through production of the vasoconstricting agent 20-HETEs in VSMCs in response to elevated arachidonic acid.[36] The contrast between our findings and those of Zonta et al[58] and Mulligan and MacVicar[36] may be explained by differences in the experimental conditions used in these studies. Mulligan and MacVicar did not stimulate the astrocytes by neuronal activation, but instead, they used released Ca^{2+} from caged Ca^{2+} in the astrocytes or applied noradrenaline. These authors indicated that arteriolar constrictions only occurred with large-amplitude Ca^{2+} changes in the astrocyte endfeet. Furthermore, unlike our study or that of Zonta et al,[58] Mulligan and MacVicar only examined nonconstricted arterioles, such that vasodilation would not be observed. It is thus possible that the astrocytes release constricting and dilating substances, and that significant astrocytic stimulation may favor the release of vasoconstricting substances. In addition, the response of the smooth muscle cells to substances released from the astrocytes would likely depend on the degree of constriction and membrane potential of the smooth muscle cells.[45] Future research on the interaction between active astrocytes and VSMCs should clarify the apparent opposite roles of astrocytes on the microvasculature.

In this study, we provide evidence suggesting that increased neuronal activity is translated into arteriolar vasodilation via multiple mechanisms. The fact that activation of mGluR alone did indeed abrogate Ca^{2+} oscillations in paren-

chymal arterioles confirms previous studies supporting a role of neuronally released glutamate and activation of astrocytic mGluR.[57] However, it is possible that the mGluR agonist also acts through the neurons. Moreover, our data indicate that mGluR antagonists do not completely suppress astrocytic Ca^{2+} responses. The residual Ca^{2+} transient in the astrocytes could be sufficient to drive suppression of parenchymal arteriolar Ca^{2+} oscillations and vasomotion. It should be noted that using EFS or FS, additional signaling molecules (eg, potassium and NO) released from the neurons could also stimulate the astrocytes or the VSMC directly. Nonetheless, our results support the important role of astrocytic $[Ca^{2+}]_i$ in coupling neuronal activity to the vasculature, and that the coupling from neurons to arterioles is rapid. Furthermore, we propose that neurovascular coupling occurs through a suppression of arteriolar Ca^{2+} oscillations, possibly through smooth muscle hyperpolarization. Abundant evidence suggests a complex bidirectional communication between astrocytes and vascular reactivity. Developing a detailed understanding of the normal physiological mechanisms that underlie this communication will serve as a foundation for understanding pathological disorders associated with the brain microcirculation, such as stroke, Alzheimer's disease, and migraine.[27]

Acknowledgments

This work was supported by National Institutes of Health grants HL44455 and HL63722 to M.T.N, a postdoctoral fellowship from the American Heart Association to J.A.F (0425923T), and by a grant from the Totman Trust for Medical Research.

References

1. Aguado F, Espinosa-Parrilla JF, Carmona MA, Soriano E. Neuronal activity regulates correlated network properties of spontaneous Ca^{2+} transients in astrocytes in situ. *J Neurosci*. 2002;22:9430–9444.
2. Akgören N, Dalgaard P, Lauritzen M. Cerebral blood flow increases evoked by electrical stimulation of rat cerebellar cortex: relation to excitatory synaptic activity and nitric oxide synthesis. *Brain Res*. 1996; 710:204–214.
3. Anderson CM, Bergher JP, Swanson RA. ATP-induced ATP release from astrocytes. *J Neurochem*. 2004;88:246–256.
4. Anderson CM, Nedergaard M. Astrocyte-mediated control of cerebral microcirculation. *Trends Neurosci*. 2003;26:340–344.
5. Barres BA, Chun LLY, Corey D. Calcium current in cortical astrocytes: induction by cAMP and neurotransmitters and permissive effect of serum factors. *J Neurosci*. 1989;9:3169–3175.
6. Brahma B, Forman RE, Stewart EE, Nicholson C, Rice ME. Ascorbate inhibits edema in brain slices. *J Neurochem*. 2000;74:1263–1270.
7. Brown LA, Key BJ, Lovick TA. Inhibition of vasomotion in hippocampal cerebral arterioles during increases in neuronal activity. *Auton Neurosci*. 2002;95:137–140.
8. Carmignoto G, Pasti L, Pozzan T. On the role of voltage-dependent calcium channels in calcium signaling of astrocytes in situ. *J Neurosci*. 1998;18:4637–4645.
9. Chaigneau E, Oheim M, Audinat E, Charpak S. Two-photon imaging of capillary blood flow in olfactory bulb glomeruli. *Proc Natl Acad Sci U S A*. 2003;100:13081–13086.
10. Cholet N, Bonvento G, Seylaz J. Effect of neuronal NO synthase inhibition on the cerebral vasodilatory response to somatosensory stimulation. *Brain Res*. 1996;708:197–200.
11. Cohen Z, Bonvento G, Lacombe P, Hamel E. Serotonin in the regulation of brain microcirculation. *Prog Neurobiol*. 1996;50:335–362.
12. Cornell-Bell AH, Finkbeiner SM, Cooper MS, Smith SJ. Glutamate induces calcium waves in cultured astrocytes: long-range glial signaling. *Science*. 1990;247:470–473.
13. D'Ascenzo M, Vairano M, Andreassi C, Navarra P, Azzena GB, Grassi C. Electrophysiological and molecular evidence of L-(Ca_v1), N-($Ca_v2.2$), and R-($Ca_v2.3$) type Ca^{2+} channels in rat cortical astrocytes. *Glia*. 2004; 45:354–363.
14. del Zoppo GJ, and Mabuchi T. Cerebral microvessel responses to focal ischemia. *J Cereb Blood Flow Metab*. 2003;23:879–894.
15. Dirnagl U, Niwa K, Sixt G, Villringer A. Cortical hypoperfusion after global forebrain ischemia in rats is not caused by microvascular leukocyte plugging. *Stroke*. 1994;25:1028–1038.
16. Fergus A, Lee KS. Regulation of cerebral microvessels by glutamatergic mechanisms. *Brain Res*. 1997;754:35–45.
17. Filosa JA, Bonev AD, Nelson MT. Calcium dynamics underlying neurovascular coupling in rat cerebral microvessels. *Society for Neurosci*. 2002;23.
18. Funk W, Itaglietta M. Spontaneous arteriolar vasomotion. *Prog Appl Microcirc*. 1993;3:66–82.
19. Goadsby PJ, Edvinsson L. Neurovascular control of the cerebral circulation. In Edvinsson L, Krause DN, eds. *Cerebral Blood Flow and Metabolism*. New York, NY: Lippincott Williams and Wilkins; 2002: 172–188.
20. Golgi C. *Sulla Fine Anatomia Degli Organi Centrali del Sisterna Nervosa*. Milano, Italy: Hoepli. 1886.
21. Gulbenkaian S, Uddman R, Edvinsson L. Neuronal messengers in the human cerebral circulation. *Peptides*. 2001;22:995–1007.
22. Haddock RE, Hill CE. Differential activation of ion channels by inositol 1,4,5-trisphosphate (IP_3)-and ryanodine-sensitive calcium stores in rat basilar artery vasomotion. *J Physiol*. 2002;545:615–627.
23. Harder DR, Zhang C, Gebremedhin D. Astrocytes function in matching blood flow to metabolic activity. *News Physiol Sci*. 2002;16:27–31.
24. Höffer T, Venance L, Giaume C. Control and plasticity of intercellular calcium waves in astrocytes: a modeling approach. *J Neurosci*. 2002;22: 4850–4859.
25. Iadecola C, Yang G, Xu S. 7-Nitroindazole attenuates vasodilation from cerebellar parallel fiber stimulation but not acetylcholine. *Am J Physiol*. 1996;270:R914–R919.
26. Iadecola C. Neurogenic control of the cerebral microcirculation: is dopamine minding the strore? *Nat Neurosci*. 1998;1:263–265.
27. Iadecola C. Neurovascular regulation in the normal brain and in Alzheimer's disease. *Nat Neurosci*. 2004;5:347–360.
28. Jensen AM, Chiu SY. Differential intracellular responses to glutamate in type 1 and type 2 cultured brain astrocytes. *J Neurosci*. 1991;11: 1674–1684.
29. Kacem K, Lacombe P, Seylaz J, Bonvento G. Structural organization of the perivascular astrocyte endfeet and their relationship with the endothelial glucose transporter: a confocal microscopy study. *Glia*. 1998; 23:1–10.
30. Kirischuk S, Matiash V, Kulik A, Voitenko N, Kostyuk P, Verkhratsy A. Activation of P_2-purino-, α_1-adreno and H_1-histamine receptors triggers cytoplasmic calcium signaling in cerebellar Purkinje neurons. *Neuroscience*. 1996;73:643–647.
31. Li N, Sul JY, Haydon PG. A calcium-induced calcium influx factor, nitric oxide, modulates the refilling of calcium stores in astrocytes. *J Neurosci*. 2003;23:10302–10310.
32. MacVicar BA, Hochman D, Dealy MJ, Weiss S. Modulation of intracellular Ca^{2+} in cultured astrocytes by influx through voltage-activated Ca^{2+} channels. *Glia*. 1991;4:448–455.
33. MacVicar BA, Tse FWT. Norepinephrine and cyclic adenosine 3′:5′-cyclic monophosphate enhance a nifedipine-sensitive calcium current in cultured astrocytes. *Glia*. 1988;1:359–365.
34. Mayhew JE, Askew S, Zheng Y, Porril J, Westby GWM, Redgrave P, Rector DM, Harper RM. Cerebral vasomotion: a 0.1-Hz oscillation in reflected light imaging of neural activity. *NeuroImage*. 1996;4:183–193.
35. Milani D, Facci L, Guidolin D, Leon A, Skaper SD. Activation of polyphosphoinositide metabolism as a signal-transducting system coupled to excitatory amino acid receptors in astroglial cells. *Glia*. 1989; 2:161–169.
36. Mulligan SJ, MacVicar BA. Calcium transients in astrocyte endfeet cause Cerebrovascular constrictions. *Nature*. 2004;431:195–199.
37. Nedergaard M, Ransom B, Goldman S. New roles for astrocytes: redefining the functional architecture of the brain. *Trends Neurosci*. 2003;26: 523–530.
38. Nilsson H, Aalkjear C. Vasomotion: mechanisms and physiological importance. *Mol Interv*. 2003;3:79–89.
39. Niwa K, Araki E, Morham SG, Ross ME, Iadecola C. Cyclooxygenase-2 contributes to functional hyperemia in whisker-barrel cortex. *J Neurosci*. 2000;20:763–770.

40. Parri R, Crunelli V. An astrocyte bridge from synapse to blood flow. *Nat Neurosci*. 2003;6:5–6.
41. Pasti L, Volterra A, Pozzan T, Carmignoto G. $[Ca^{2+}]_i$ oscillations in astrocytes triggers repetitive glutamate-mediated $[Ca^{2+}]_i$ increases in neurons in situ. *J Neurosci*. 1997;17:7817–7830.
42. Paulson OB, and Newman EA. Does the release of potassium from astrocyte endfeet regulate cerebral blood flow? *Science*. 1987;237: 896–898.
43. Pearce B, Albrecht J, Morrow C, Murphy S. Astrocyte glutamate receptor activation promotes inositol phospholipids turnover and calcium influx. *Neurosci Lett*. 1986;72:335–340.
44. Peng X, Carhuapoma JR, Bhardwaj A, Alkayed NJ, Falck JR, Harder DR, Traystaman RJ, Koehler RC. Suppression of cortical functional hyperemia to vibrissal stimulation in the rat by epoxygenase inhibitors. *Am J Physiol Heart Circ Physiol*. 2002;283:H2029–H2037.
45. Peppiatt C, Attwell D. Feeding the brain. *Nature*. 2004;431:137–138.
46. Peters O, Schipke CG, Hashimoto Y, Kettenmann H. Different mechanisms promote astrocyte Ca2+ waves and spreading depression in the mouse neocortex. *J Neurosci*. 2003;23:9888–9896.
47. Pin J.-P, Duvoisin R. The metabotropic glutamate receptors: structure and functions. *Neuropharmacology*. 1995;34:1–26.
48. Porter JA, McCarthy KD. GFAP-positive hippocampal astrocytes *in situ* respond to glutamatergic neuroligand with increased in $[Ca^{2+}]_i$. *Glia*. 1995;13:101–112.
49. Roy CS, Sherrington CS. On the regulation of the blood supply of the brain. *J Physiol*. 1890;11:85–108.
50. Sala L. Zur feineren anatomie des grossen Seepferdefusses. *Zeitschr Wissenschaftl Zool*. 1891;1:18–45.
51. Simard M, Arcuino G, Takano T, Liu QS, Nedergaard M. Signaling at the gliovascular interface. *J Neurosci*. 2003;23:9254–9262.
52. Tsai AG, Intaglietta M. Evidence of flowmotion induced changes in local tissue oxygenation. *Int J Microcirc Clin Exp*. 1993;12:75–88.
53. Vaucher E, Hamel E. Cholinergic basal forebrain neurons project to cortical microvessels in the rat: electron microscopic study with anterogradely transported *Phaseolus vulgaris* leucoagglutinin and choline acetyltransferase immunocytochemistry. *J Neurosci*. 1995;15:7427–7441.
54. Wienchen AE, Casagrande VA. Endothelial nitric oxide synthase (eNOS) in astrocytes: another source of nitric oxide in neocortex. *Glia*. 1999;26: 280–290.
55. Yuste R, Lanni F, Konnerth A. *Imaging Neurons: A Laboratory Manual*. Cold Spring Harbor, NY: Cold Spring Harbor Press; 1999:34.1–34.9.
56. Zang C, Harder DR. Cerebral capillary endothelial cell mitogenesis and morphogenesis induced by astrocytic epoxyeicosatrienoic acid. *Stroke*. 2002;33:2957–2964.
57. Zonta M, Angulo MC, Gobbo S, Rosengarten B, Hossmann K-A, Pozzan T, Carmignoto G. Neuron-to-astrocyte signaling is central to the dynamic control of brain microcirculation. *Nat Neurosci*. 2002;6:43–50.
58. Zonta M, Sebelin A, Gobbo S, Fellin T, Pozzan T, Carmignoto G. Glutamate-mediated cytosolic calcium oscillations regulate a pulsatile prostaglandin release from cultured rat astrocytes. *J Physiol*. 2003;553: 407–414.